JACS
JOURNAL OF THE AMERICAN CHEMICAL SOCIETY

Article

pubs.acs.org/JACS

A Cyanine Dye to Probe Mitophagy: Simultaneous Detection of Mitochondria and Autolysosomes in Live Cells

Ying Liu,[†,‡,#] Jin Zhou,[†,⊥,#] Linlin Wang,[†,‡,#] Xiaoxiao Hu,[§] Xiangjun Liu,[†] Meirong Liu,[†] Zehui Cao,[†] Dihua Shangguan,[*,†,‡] and Weihong Tan[§,∥]

[†]Beijing National Laboratory for Molecular Sciences, Key Laboratory of Analytical Chemistry for Living Biosystems, Institute of Chemistry, Chinese Academy of Sciences, Beijing, 100190, China

[‡]University of the Chinese Academy of Sciences, Beijing 100049, China

[§]Molecular Science and Biomedicine Laboratory, State Key Laboratory of Chemo/Bio-Sensing and Chemometrics, College of Biology and College of Chemistry and Chemical Engineering, Hunan University, Changsha, 410082, China

[∥]Department of Chemistry, Center for Research at the Bio/Nano Interface, Health Cancer Center, UF Genetics Institute, McKnight Brain Institute, University of Florida, Gainesville, Florida 32611-7200, United States

[⊥]CAS Center for Excellence in Nanoscience, National Center for Nanoscience and Technology, Beijing, 100190, China

Supporting Information

ABSTRACT: Mitophagy is a process in which cells remove dysfunctional mitochondria and recycle their constituents in a lysosome-dependent manner. To probe this process, two different fluorescent dyes specific for mitochondria and lysosomes, respectively, are often used in combination. However, current fluorescent dyes for lysosomes cannot distinguish mitochondria-containing autolysosomes from other lysosomes. Therefore, we herein report a cyanine dye, HQO, which can simultaneously probe mitochondria and autolysosomes in live cells by exhibiting different fluorescence properties. HQO selectively accumulates in mitochondria but then transforms to the protonated $HQOH^+$ form with the decrease of pH when dysfunctional mitochondria evolve into autolysosomes. Since HQO and $HQOH^+$ exhibit different absorption and emission with Ex/Em at 530/650 and 710/750 nm, respectively, in a low polarity environment, such as that found in micelles, they are uniquely suited to monitor mitophagy with the ability to distinguish autolysosomes from other lysosomes.

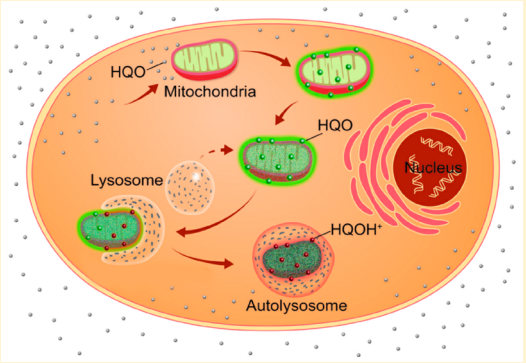

INTRODUCTION

Mitochondria are cellular powerhouses. In addition to supplying cellular energy, they are involved in many other important metabolic processes, such as storage of calcium ions, signaling and cellular differentiation, growth, apoptosis, and death.[1] They are also the major source of cellular reactive oxygen species (ROS), which, in turn, can cause oxidative damage to mitochondria. The accumulation of mitochondrion damage is believed to be associated with aging, cancer, and neurodegenerative diseases.[2] Therefore, maintaining a healthy population of mitochondria is essential for cell survival. Inside the cell, damaged and excess mitochondria are selectively eliminated through an autophagy (mitophagy) process in order to maintain mitochondrial quality and quantity.[1d,3] This process involves lysosomes, which are acidic organelles (pH 4.5−5.5) in charge of waste disposal, and capable of breaking down many types of waste materials, including proteins, nucleic acids, carbohydrates, lipids, and cellular debris.[4] Mitophagy is a special form of autophagy by which the cell removes dysfunctional mitochondria and recycles their constituents in a lysosome-dependent manner. During mitophagy, damaged mitochondria are selectively enclosed in autophagosomes (mitophagosomes), which subsequently fuse with nearby lysosomes to form autolysosomes (or mitolysosomes, i.e., mitochondria-containing autolysosomes), where the mitochondrial components get degraded.[1d,3,5] Probes for monitoring the occurrence of mitophagy in live cells can provide deep insights into mitochondrion metabolism and serve as powerful tools for the screening of inhibiting or inducing agents of mitophagy.

Most of the current methods for monitoring autophagy are based on the detection of protein markers using antibodies or fluorescent protein tags.[3,5a,b,6] Although these methods have achieved some success in monitoring the mitophagy process, few of the protein markers are particularly specific for mitophagy. In addition, antibody-based detection is hard to carry out in live cells. To solve these problems, fluorescent small molecules specific for mitochondria or lysosomes, e.g., LysoTracker Red and MitoTracker Green,[7] have been employed to probe mitophagy. Most recently, two-photon

Received: April 20, 2016
Published: August 30, 2016

DOI: 10.1021/jacs.6b04048
J. Am. Chem. Soc. 2016, 138, 12368−12374

excitation fluorescence imaging of mitochondria and lysosomes with two different probes also showed good performance for mitophagy investigation.[8] While these methods are usually effective, two fluorescent dyes are required for simultaneous detection of mitochondria and lysosomes.[5b,7] In addition, current lysosome probes are not specific only for mitochondria-containing autolysosomes but can also stain lysosomes involved in other intracellular processes such as phagocytosis and endocytosis. A single fluorescent molecule that can be used to detect mitochondria and lysosomes simultaneously, and is highly specific for mitochondria-containing autolysosomes, would provide a new approach to mitophagy study with unprecedented simplicity and accuracy.

Here, we report a cyanine dye, 2,6-bi(2-(3,3-dimethyl-1-propylindolin-2-ylidene)ethylidene)-cyclohexanone (HQO), which can be used for simultaneous observation of mitochondria and autolysosomes in live cells using microscopy. HQO specifically accumulates in mitochondria at physiological pH with excitation/emission wavelengths at 530/650 nm. When damaged mitochondria fuse with lysosomes to form autolysosomes, the pH decrease within the autolysosomes induces protonation of HQO (to $HQOH^+$), resulting in its wavelengths redshifting to 710/750 nm (Figure 1).

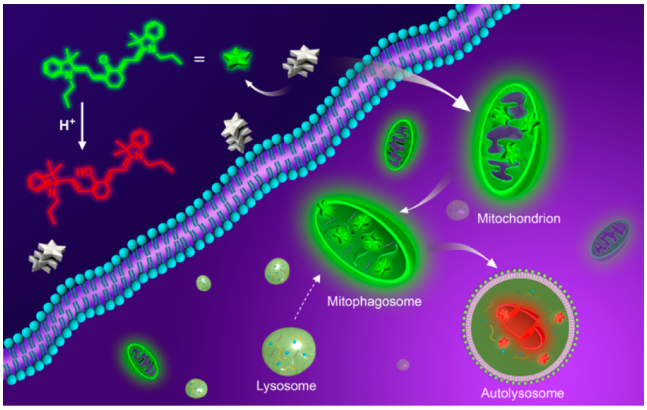

Figure 1. Schematic representation of the mitophagy process probed by HQO.

RESULTS AND DISCUSSION

In order to probe the mitophagy process with a single dye, the fluorescent dye needs to be highly specific for mitochondria and mitochondria-containing autolysosomes. Compared to mitochondria, autolysosomes have a lower interior pH in the range 4.5−5.5, which is optimal for acid hydrolase enzymes to digest dysfunctional mitochondria. Therefore, an ideal dye would be able to respond to the lower pH of autolysosomes with corresponding changes in fluorescence. IR780 is a near-infrared heptamethine dye that can selectively accumulate in mitochondria in tumor cells.[9] It was chosen as the parent molecule to create a dye molecule with the desired properties. Modifications of IR780 yielded a product whose absorption and emission spectra changed significantly in the presence of sodium dodecyl sulfate (SDS). This product was identified as HQO by ^{1}H NMR, ^{13}C NMR, and HRMS before further confirmation by synthesis (Scheme S1). HQO was reported to be a pH-sensitive dye whose basic form (ketone structure) exhibits absorption in the visible region (λ_{max} = 475 and 515 nm), while the acidic form (enol structure, $HQOH^+$) exhibits absorption in the near-infrared region (λ_{max} = 710 nm).[10] Because of its low solubility and aggregation in aqueous solutions, HQO has been poorly characterized and found few applications. However, we suspected that the low water solubility might make HQO suitable for probing pH changes in a lipid environment, such as biological membranes. The spectral characteristics of HQO in response to pH changes were therefore investigated to test our hypothesis.

HQO shows a broad absorption band in the range 420−580 nm (Figure S1). The molar extinction coefficients of HQO in organic solvents (ε_{max} = (6.2−7.8) × 10^4) are much higher than those in H_2O and HEPES buffer (ε_{max} = (3.6−4.3) × 10^4) (Table S1), suggesting less aggregation of HQO in organic solvents. The addition of 10 mM HCl in DMSO caused the absorption peak of HQO to shift to 710 nm, accompanied by a significant increase (ε_{max} = 1.4 × 10^5) (Figure 2b), which could be attributed to the transformation from HQO to $HQOH^+$

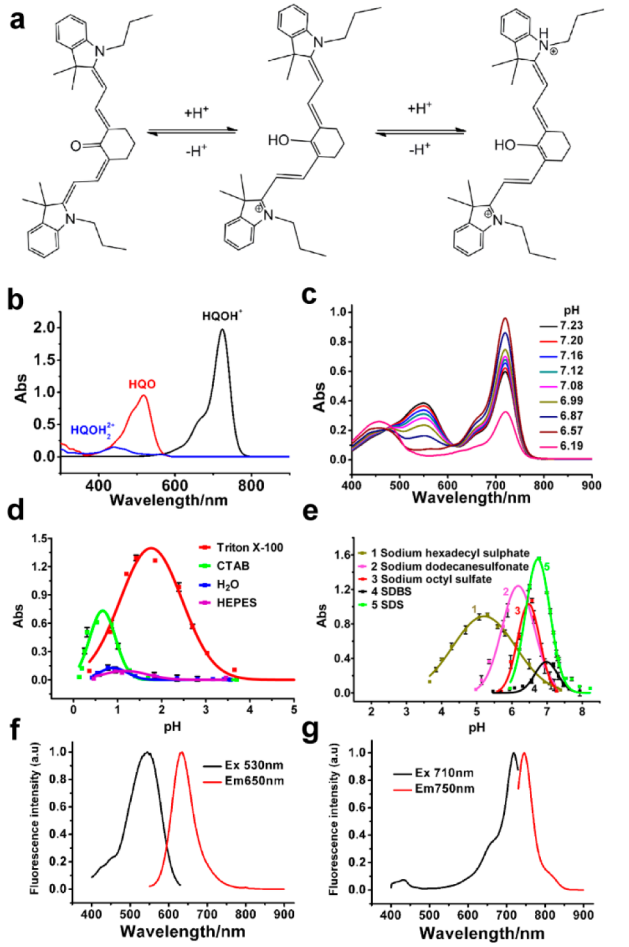

Figure 2. (a) Structural transformation of HQO, $HQOH^+$, and $HQOH_2^{2+}$. (b) Absorption spectra of HQO (11.5 μM) in DMSO containing different concentrations of HCl: HQO (no HCl), $HQOH^+$ (10 mM HCl), and $HQOH_2^{2+}$ (500 mM HCl). (c) Absorption spectra of HQO in 10 mM SDS at different pHs. (d, e) Changes in absorbance of HQO (11.5 μM) at 710 nm in different solutions with different bulk pHs, including 10 mM SDS, 1.5 mM Triton X-100, 3 mM CTAB, 150 mM sodium octyl sulfate, 20 mM SDBS, 3 mM sodium hexadecyl sulfate, and 10 mM sodium 1-dodecanesulfonate in HEPES buffer. The CMCs of the surfactants are shown in Table S3. (f, g) Excitation and emission spectra of HQO (5 μM) in SDS solution at pH 8.23 (f) and pH 6.59 (g).

DOI: 10.1021/jacs.6b04048
J. Am. Chem. Soc. 2016, 138, 12368−12374

form.[10] The significant redshift of the absorption spectra of $HQOH^+$ may be a result of the formation of the pull−push π-conjugation system in the cyanine dye.[10a] However, further increase of HCl to 500 mM caused disappearance of the absorption peak at 710 nm and the emergence of a small peak at 430 nm. This could be explained by the further protonation at the nitrogen of the indole ring, resulting in $HQOH_2^{2+}$ (Figure 2a,b), which led to disruption of the large π-conjugation system. The ^1H NMR titration in DMSO showed that the chemical shift of the alkene and aromatic protons of HQO continuously increased with the addition of HCl until the ratio of HQO to HCl reached 1:2 (Figure S2), which further confirmed the double protonation of HQO. Notably, the changes in the absorption spectra of HQO were reversible when NaOH was added.

In order to investigate the spectral behavior of HQO in a lipid environment, different micelles were used, including SDS (anionic surfactant), CTAB (cationic surfactant), and Triton X-100 (nonionic surfactant). Unlike in buffer or organic solvents, HQO in SDS solution showed two bands, one in the range 420−580 nm and the other with maximum absorption at 710 nm (Figures 2c, S1c, and S3). In contrast, HQO in other micelle solutions showed only an enhanced absorption band within 420−580 nm but no absorption at 710 nm, which was also visible by different colors of HQO in SDS, CTAB, or Triton X-100 solution (Figure S3). Some common inorganic ions were also tested but did not display a notable influence on the absorption of HQO in buffer (Figure S4). The changes in the absorption spectra of HQO induced by various pH values were further measured by titration with HCl. As shown in Figure 2c, with the addition of HCl to SDS solution, the absorption peak at 710 nm rose first, accompanied by the decrease of the band at 420−580 nm. Then, with further addition of HCl, the peak at 710 nm declined, while the peak at 430 nm increased ($HQOH_2^{2+}$ formed). Similar trends of spectral change were observed with the continuous addition of HCl into Triton X-100, CTAB, and DMSO solutions (Figure S5). The isoabsorptive points in those figures indicate three distinct forms of HQO present at equilibrium. These results confirmed that the spectral changes resulted from the transformation between different HQO forms under different pH conditions.

The pH titration curves of HQO in buffer and seven micelle solutions were then constructed on the basis of the absorbance at 710 nm (Figure 2d,e), and the apparent pK_{a1} and pK_{a2} of $HQOH_2^{2+}$ are shown in Table S1. Interestingly, in anionic micelle solutions, the apparent pK_a values (4.0−7.3) are much higher than those in water, buffer, CTAB, or Triton X-100 solution (0−2.4). Since the interface of anionic micelles is highly negatively charged, the electrostatic attraction between the interface and protons (H^+) caused the local pH (density of protons) at the vicinity of the interface to be considerably lower by several pH units compared to that in bulk solution.[11] This enrichment of protons at the micelle interface might have contributed to the seemingly much higher bulk pH during HQO transformation in anionic micelle solution (Figure S6). In water or HEPES buffer, titration curves showed a very low peak in the pH range 0.5−1.4, which suggests that the real pK_{a1} and pK_{a2} of $HQOH_2^{2+}$ may be in this range. The low absorbance at 710 nm in aqueous solutions may result from the aggregation of $HQOH^+$ in these solutions. The slightly lower apparent pK_a values of HQO in CTAB solution (1.18, 0.25) than that in aqueous solutions (1.38, 0.55) indicates a higher local pH of HQO in CTAB micelles than in bulk solution. Similarly, the slightly higher apparent pK_a values in Triton X-100 solution (2.36, 0.92) compared to aqueous solutions suggests a slightly lower local pH as a result of the hydroxyl headgroup of Triton X-100. Noticeably, the peak shape of titration curves and apparent pK_a values of HQO in five anionic micelle solutions were all different, which might be due to the fact that HQO was present in different microenvironments formed by different anionic surfactants.

While neither HQO nor $HQOH^+$ showed significant fluorescence in buffer, they emitted strongly fluorescence in SDS solution (Figure 2f,g, Figure S7). At pH 8.23, HQO showed an excitation peak at 530 nm and an emission peak at 650 nm, corresponding to the excitation and emission of the HQO form. At pH 6.59, HQO showed an excitation peak at 710 nm and an emission peak at 750 nm, corresponding to the excitation and emission of the $HQOH^+$ form. Unlike many other pH-sensitive dyes that respond to pH by simple changes in intensity, HQO displays strong fluorescence with significant wavelength shift at different pHs. The fluorescence quantum yields of HQO/$HQOH^+$ in SDS solution and DMSO were measured as 0.21/0.08 and 0.40/0.31, respectively. This unique property, coupled with its minimum fluorescence in aqueous buffer, makes HQO especially suitable for fluorescence-based detection in live cells.

The cytotoxicity of HQO against MCF-7 cells was investigated by CCK-8 assay (Figure S8). After incubation of MCF-7 cells with different concentrations of HQO for 24 h, no significant cytotoxicity was observed even with a concentration up to 100 μM. This result suggests that HQO has the potential to be used as a safe fluorescent probe for monitoring dynamic processes in live cells.

The localization of HQO in cells was tested by costaining of live cells with HQO and WGA (wheat germ agglutinin, a plasma membrane probe), MitoTracker Green (mitochondrion probe), LysoTracker Blue (lysosome probe), BODIPY FL C5-Ceramide (Golgi- Tracker), or BODIPY FL Glibenclamide (endoplasmic reticulum (ER)-Tracker) (Figures 3 and S9). Confocal images show that the fluorescence of HQO (Ex 559 nm) almost completely overlaid with that of MitoTracker Green. The overlap coefficient (OLC) and Pearson's correlation coefficient (PCC) were 0.94 and 0.93, respectively. In contrast, HQO did not significantly stain other plasma membranes, lysosome, or golgi, with OLC and PCC values lower than 0.45 and 0.35, respectively. The fluorescence of HQO partly overlaid with that of ER tracker, with OLC and PCC values at 0.79 and 0.68, respectively. The large area of ER was not stained by HQO, suggesting that HQO is a poor stain for ER. These images indicate that HQO very likely accumulated in mitochondria selectively. This conclusion was further confirmed by treatment of cells with carbonyl cyanide 4-(trifluoromethoxy) phenylhydrazone (FCCP), an uncoupler of mitochondrial oxidative phosphorylation. After treatment with FCCP, the fluorescence of HQO in cells was greatly reduced (Figure S10), suggesting that the high selectivity of HQO for mitochondria may be related to mitochondrial transmembrane potential or energy metabolism.

The localization of $HQOH^+$ as compared to HQO was tested in cells costained with LysoTraker Blue and cells transfected by the plasmid of GFP-LAMP1 (lysosomal-associated membrane protein 1) (Figure 4). After incubation of HQO with cells in serum-free medium for 1−1.5 h, the $HQOH^+$ fluorescence (Ex = 635 nm) seemed to largely overlay with only a small portion

DOI: 10.1021/jacs.6b04048
J. Am. Chem. Soc. 2016, 138, 12368−12374

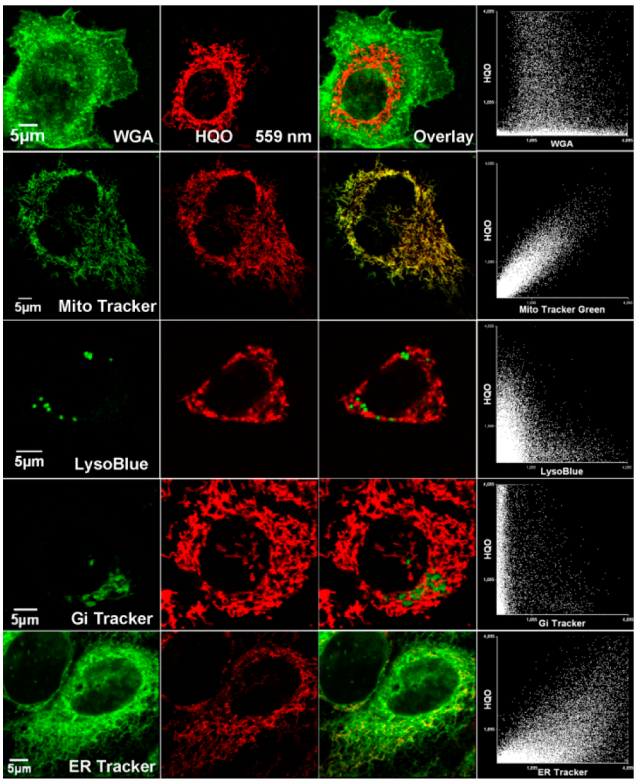

Figure 3. Fluorescence imaging of cells costained with HQO (20 μM) and WGA (plasma membrane probe, LoVo cell), MitoTracker Green (MCF-7 cell), LysoTraker Blue (LoVo cell), Golgi-Tracker (MCF-7 cell), or ER-Tracker (MCF-7 cell). Cells were incubated with dyes at 37 °C for 30 min in serum-free medium, and then washed before confocal imaging. Probes are indicated on each fluorescent image. Plots in the last column represent the intensity correlation plot of HQO and probes.

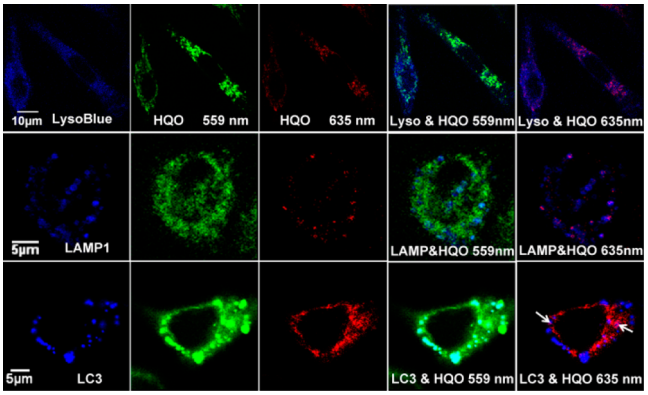

Figure 4. Fluorescence imaging of LoVo cells stained with HQO (20 μM). Top, cells costained with LysoTracker Blue (ex = 405 nm); middle, cells transfected by GFP-LAMP1 plasmid; bottom, cells transfected by GFP-LC3A plasmid. Cells were incubated with HQO at 37 °C for 1 h (top), 1.5 h (middle), or 2 h (bottom) in serum-free medium, and then washed before confocal imaging.

of the LysoTraker Blue-stained or GFP-LAMP1 positive areas, indicating that $HQOH^+$ only labeled part of the lysosome. These staining behaviors of HQO and $HQOH^+$ were also observed in other cellular experiments (Figures S11–S14). The fluorescence of $HQOH^+$ was observed within the regions of mitochondria, especially those with a high density of mitochondria, providing the first clue that $HQOH^+$ may be able to label autolysosomes derived from mitophagy, since the regions of high density mitochondria could also contain a higher number of damaged and/or excessive mitochondria that could lead to mitophagy.

During mitophagy, damaged mitochondria are first enclosed in mitophagosomes, followed by mitophagosomes fusing with lysosomes to form autolysosomes. To investigate whether HQO could label mitophagosomes, cells transfected with GFP-LC3A (autophagosomal marker) plasmid were stained by HQO. After growing in serum-free medium for 2 h, all patches of GFP fluorescence coexisted with HQO fluorescence, suggesting that HQO can also label mitophagosomes. In comparison, only a few GFP fluorescence spots (arrowheads) overlapped with the fluorescence of $HQOH^+$, which can suggest that GFP-LC3A became degraded and that the GFP fluorescence had been weakened in the acidic autolysosome as reported elsewhere.[6d]

In order to further demonstrate the selectivity of $HQOH^+$ for mitochondria-containing autolysosomes, a bafilomycin A treatment experiment was performed. Bafilomycin A is an inhibitor of vacuolar H^+-ATPase, which blocks the acidification of lysosomes, and subsequently prevents fusion between autophagosomes and lysosomes.[12] After incubation of LoVo cells with HQO and bafilomycin A in serum-free media for 2 h, the fluorescence of $HQOH^+$ in bafilomycin A-treated cells was much weaker than that in nontreated cells. In contrast, the fluorescence of HQO in bafilomycin A-treated cells was brighter than that in nontreated cells (Figure S15). These findings further confirm that $HQOH^+$ selectively labeled autolysosomes, whose formation was disrupted by bafilomycin A.

On the basis of our pH titration curves of HQO in water, buffer, CTAB, and Triton X-100 solutions, its pK_{a1} and pK_{a2} are in the low 0–2.0 range, which does not agree with the reported pK_{a2} of 4.5[10b] or 6–7.[10c] This low pK_a may not seem feasible for applications under physiological conditions. However, as we have shown earlier with anionic micelles, microenvironments surrounding certain membrane structures could provide sufficiently low local pH for the HQO/$HQOH^+$ transition to happen. It is well-known that both sides of the biological membrane surface are negatively charged in most cases because of the bilayer phospholipid structure. Thus, the local pH of the biological membrane surface may be lower than the pH of the bulk solution. Different biological membranes or even different regions on a membrane may have different local pHs, depending on the density of net negative charge. Mitochondria usually have higher negative transmembrane potentials (−120 to −180 mV) than other membranes in cells (−40 to −80 mV).[9a,13] The inner mitochondrial membrane contains a marker anionic phospholipid called cardiolipin, which constitutes about 20% of the total lipid composition. Cardiolipin has a dimeric structure with four acyl chains and two ionizable phosphate groups.[14] This higher anionic phospholipid content could further lead to a lower local pH of the mitochondrial membrane compared to other biological membranes. These unique features of the mitochondrial membrane may have contributed to the high selectivity of HQO/$HQOH^+$ for mitochondria/mitochondria-containing autolysosomes.

Additional tests were conducted to confirm that HQO/$HQOH^+$ could be used to track mitophagy. It is well-known that nutrient starvation can induce autophagy in cultured cells and in intact organisms.[5a,6d] Therefore, MCF-7 cells were incubated with HQO and LysoTracker Blue in serum-free

DOI: 10.1021/jacs.6b04048
J. Am. Chem. Soc. 2016, 138, 12368–12374

medium and normal culture medium with different incubation times (Figure 5). Confocal imaging showed that the

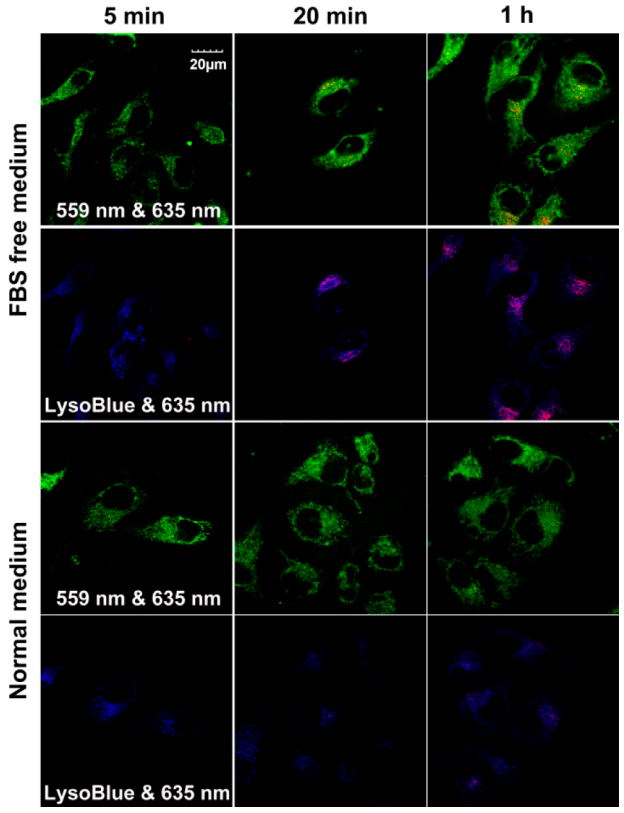

Figure 5. Overlaid confocal images of MCF-7 cells incubated with HQO (10 μM, Ex, 559 or 635 nm) and LysoTracker Blue (10 μM, Ex, 405 nm) in serum-free medium or normal medium for different times. Cells were washed before imaging.

fluorescence of $HQOH^+$ in cells increased with prolonged incubation time from 5 min to 1 h, while the fluorescence of HQO and LysoTracker Blue remained largely unchanged. The regions stained by $HQOH^+$ were also mostly within the areas stained by HQO and LysoTracker Blue. The increase of $HQOH^+$ fluorescence in cells cultured in serum-free medium was much more significant than that in cells cultured in normal medium, suggesting that $HQOH^+$ fluorescence could be linked to nutrient starvation induced mitophagy. In addition, the fluorescence of LysoTracker Blue was observed in cells after a 5 min culture, but only very weak fluorescence of $HQOH^+$ was observed at that time. Similar results were also obtained in the experiment with GFP-LAMP1 plasmid transfected cells (Figure S16). We also treated MCF-7 cells with liensinine (mitophagy inhibitor)[15] and rapamycin (mitophagy inducer),[6c] respectively, which were then incubated with HQO for different times in normal medium to study mitophagy. Confocal imaging showed significant enhancement of $HQOH^+$ fluorescence in rapamycin-treated cells but almost no $HQOH^+$ fluorescence from liensinine-treated cells (Figure S17). These results suggest that $HQOH^+$ selectively stains autolysosomes derived from damaged mitochondria, not other lysosomes in the cell.

In order to further understand the interaction of HQO with cells, a real-time live-cell imaging experiment was performed in serum-free medium with addition of HQO. As shown in Figures 6 and S18, HQO was observed to enter cells and locate in mitochondria within 5 min, and the fluorescence of HQO

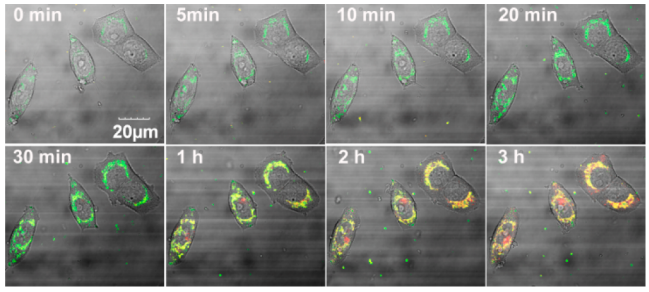

Figure 6. Real-time confocal imaging of MCF-7 cells incubated with HQO (20 μM) in serum-free medium. All pictures are overlaid images of optical images and fluorescence images excited at 559 and 635 nm.

slightly increased with time (cells not washed). The fluorescence of $HQOH^+$ was not observed in the cells until 30 min, and became stronger with time until all HQO stained regions turned to $HQOH^+$ fluorescence at 3 h. Some cells were found to shrink and become smaller at 4 h, suggesting cell damage or death. These images revealed the mitophagy process in live cells and in real time with a single fluorescent dye.

CONCLUSION

In summary, a cyanine dye, HQO, is protonated to form $HQOH^+$ and $HQOH_2^{2+}$ at low pH (0−2.0). This transition can take place on anionic micelles or biological membrane surfaces under physiological conditions as a result of low local pH. HQO and $HQOH^+$ in anionic micelles exhibit strong absorption and emission at 530/650 and 710/750 nm, respectively. HQO selectively accumulates in mitochondria and exhibits strong fluorescence by 559 nm excitation. During mitophagy, when damaged mitochondria evolve into autolysosomes, HQO is transformed into $HQOH^+$ because of decreased pH and exhibits strong fluorescence by 635 nm excitation. $HQOH^+$ has been shown to be present only in mitochondria-containing autolysosomes but not in other lysosomes. Given these distinctive features, HQO/$HQOH^+$ can be uniquely useful as a novel fluorescent probe to investigate the mitophagy process and screen agents that either inhibit or induce mitophagy.

MATERIALS AND METHODS

Materials. IR-780, sodium acetate, bafilomycin A, liensinine, and rapamycin were obtained from J&K Chemical Technology Company, Ltd. (Beijing, China). Sodium hexadecyl sulfate and sodium octyl sulfate were from Alfa Aesar. Sodium dodecyl sulfate (SDS) was from Sigma-Aldrich. Sodium 1-dodecanesulfonate, sodium dodecylbenzenesulfonate (SDBS), and hexadecyl trimethylammonium bromide (CTAB) were from China National Pharmaceutical Group Corporation (Beijing, China). Triton X-100 was from Acros Organics. LAMP1 (NM_005561) Human ORF Clone ((GFP-tagged)-Human lysosomal-associated membrane protein 1, RG219208) and MAP1LC3A (NM_032514) Human cDNA ORF Clone ((GFP-tagged)-Human microtubule-associated protein 1 light chain 3 alpha, RG202222) were from OriGene Technologies Inc. BODIPY FL C5-Ceramide (Golgi-Tracker) and BODIPY FL Glibenclamide (ER-Tracker Green) were from Thermo Fisher Scientific. Carbonyl cyanide 4-(trifluoromethoxy) phenylhydrazone (FCCP) and FITC conjugate Wheat germ agglutinin (WGA) were from SIGMA-Aldrich. LysoTracker Blue and MitoTracker Green were from KeyGEN BioTECH (Beijing, China). Lipofectamine 3000 transfection reagent was obtained from Life Technologies. Stock solution of HQO (10 mM) was prepared in DMSO. HEPES buffer was prepared with deionized water purified using a UPHWIII-90T UP water purification system (Chengdu, China). Interactions of HQO with different surfactant

DOI: 10.1021/jacs.6b04048
J. Am. Chem. Soc. 2016, 138, 12368−12374

micelles were studied in HEPES buffer (pH 7.35, 20 mM) or deionized water.

Cell Culture. MCF-7 (human breast adenocarcinoma cell line), A549 (nonsmall cell lung cancer cell line), LoVo (human colonic carcinoma cell line), and HeLa (cervical carcinoma cell line) were purchased from Cell Resource Center of Shanghai Institute for Biological Sciences (Chinese Academy of Sciences, Shanghai, China). A549 and LoVo cells were cultured in RPMI-1640 medium (Corning). MCF-7 cells were propagated in Dulbecco's Modified Eagle's Medium (DMEM, Corning). Unless otherwise stated, the basic media were supplemented with 10% fetal bovine serum (FBS, Corning) and 1% penicillin/streptomycin (Hyclone). All cells were cultured in a humidified incubator at 37 °C and 5% CO_2.

Instruments. ^{1}H NMR spectra were recorded at 400 MHz and ^{13}C NMR spectra were recorded at 100 MHz, respectively, on a Bruker Model Avance DMX 400 Spectrometer with tetramethylsilane (TMS) as the internal standard. J values were given in hertz. High-resolution mass spectra were obtained on a Bruker Daltonics Flex-Analysis instrument. Confocal imaging was done using an OLYMPUS FV1000-IX81 confocal laser-scanning microscope (Olympus Corporation, Japan). The absorption spectra were all recorded on a UV-1800 UV−visible Spectrophotometer (UV−vis) (Japan Shimadzu Corporation) with a 10 mm light path cuvette. Fluorescence spectra were recorded on a HITACHI F-4600 Fluorescence Spectrophotometer (Hitachi Limited, Japan).

Synthesis of HQO. The synthetic route of HQO is shown in Scheme S1. HQO was obtained by treatment of 1.34 g of cyanine dye (IR-780) with 0.38 g of sodium acetate in DMF at 80 °C for 5 h. Then, HQO was purified by RP-HPLC using pure methanol for isocratic elution. A yield of about 70% was obtained.[10b] The chemical structure of HQO was characterized by ^{1}H NMR, ^{13}C NMR, and HRMS. ^{1}H NMR (400 MHz, DMSO): δ (ppm) 7.88 (d, J = 13.2 Hz, 2H), 7.28 (d, J = 7.2 Hz, 2H), 7.14 (d, J = 7.6 Hz, 2H), 6.86 (m, 4H), 5.44 (d, J = 13.2 Hz, 2H), 3.69 (t, J = 7.2 Hz, 4H), 3.12 (d, J = 5.2, 1H), 2.47 (d, J = 11.2, 3H), 1.66 (m, 2H), 1.61 (m, 4H), 1.52 (s, 12H), 0.88 (t, J = 7.6, 6H). ^{13}C NMR (75 MHz, DMSO): δ (ppm) 184.9, 162.2, 144.5, 139.2, 132.4, 128.3, 126.2, 122.2, 120.8, 107.8, 92.6, 46.4, 43.5, 28.7, 25.8, 19.7, 11.8. ESI HRMS exact mass calculated for $C_{36}H_{45}N_2O$ ($[M + H]^+$) is m/z 521.35345, compared to the measured m/z of 521.35264.

Spectral Measurement. Absorption spectra of HQO in different solvents: The concentration of HQO was fixed at 11.5 μM. HQO stock solution was dissolved in different solvents to a final volume of 400 μL, and the absorption spectra were recorded immediately at room temperature.

Absorption spectra of HQO in the presence of different surfactants: 4.6 μL of stock solution of HQO (10 mM) was mixed with different surfactants in HEPES buffer or water to a final volume of 400 μL with a final concentration of 11.5 μM. The absorption spectra were measured after sitting in the dark for 1 h at room temperature.

The pH Titration Curve and Determination of pK_a. pK_a is defined as $pK_a = pH + \log[(A_{HB} - A)/(A - A_{B^-})]$, where, A_{HB}, A, and A_{B^-} represent the absorbance of the absolute acid form, the absorbance at a chosen pH, and the absorbance of the absolute base form, respectively. The pH titration curve was plotted using the absorbance at 710 nm vs pH. The calculation of apparent pK_a value was performed with OriginPro 8.5.1 software (OriginLab, Northhampton, MA), using the "Dose Response" fitting function as $y = A_1 + (A_2 - A_1)/(1 + 10^{(\log x_0 - x)*P})$. On the basis of the calculated equation of pK_a, $\log x_0$ corresponds to the pK_a value.

Excitation and Emission Spectra of HQO in SDS Solution of Different pH. SDS (10 mM) solutions were prepared in HEPES buffer at pH 8.23 and 6.59, respectively. HQO (5 μM) was added to the SDS solutions and left to sit in the dark for 1 h at room temperature. Excitation and emission spectra were measured at Em/Ex = 650/530 nm for pH 8.23 solution and at Em/Ex = 750/710 nm for pH 6.59 solution.

Measurement of Fluorescence Quantum Yields. The fluorescence quantum yields of HQO/HQOH$^+$ were obtained on an Edinburgh Instruments FLS980 instrument. Under certain excitation wavelengths, fluorescence spectra of HEPES buffer, SDS solution, and DMSO were measured first as a baseline, and following that, fluorescence spectra of HQO in these solutions were measured. Quantum yields were calculated using F900 advanced software.

Cytotoxicity Assay. Cytotoxicity assays were carried out using MCF-7 cells. Cell viability was determined using CCK8 assay. 5000 cells per well were seeded in a 96-well plate and incubated for 12 h in a humidified incubator for adherence. HQO dissolved in DMSO was added to cells at the final concentration of 1, 10, 20, 30, 50, 70, and 100 μM and incubated for 24 h. CCK-8 reagent diluted by DMEM (FBS free) medium (10%) was added to each well after the removal of culture media and incubated for 0.5 h. Following that, the absorbance was measured at 450 nm on a plate reader (Spectra Max M5, Molecular Devices, Sunnyvale, CA). Cell viability rate was determined as $VR = (A - A_0)/(A_s - A_0) \times 100\%$, where A is the absorbance of the experimental group, A_s is the absorbance of the control group (DMSO was used as the control), and A_0 is the absorbance of the blank group (no cells).

Transient Transfection of GFP-LAMP1 or GFP-LC3A Plasmid. Briefly, 5×10^5 cells were seeded to 70−90% confluent in confocal dishes. Four μL of Lipofectamine 3000 reagent was diluted in 125 μL of Opti-MEM Medium, and vortexed for 2−3 s. A master mix of plasmid DNA was prepared by diluting 5 μg of DNA in 125 μL of Opti-MEM Medium, then adding 10 μL of P3000 reagent, and mixing well. Diluted DNA was added to the tube of diluted Lipofectamine 3000 reagent, and incubated for 5 min at room temperature. The DNA−lipid complex was then added to the cells in the confocal dishes. Cells were incubated for 2−4 days at 37 °C before usage.

Confocal Imaging of Cells Stained by Dyes. Cells were seeded in confocal glass bottom dishes with 10^5 cells per dish and cultured for 24 h. HQO and/or probes were added to each dish and cultured for different times. Cells were then washed with PBS (pH 7.4) three times, and 1 mL of culture media was finally added before imaging. Cells were imaged with a 100× objective lens. The fluorescence of LysoTracker Blue was excited with a 405 nm laser with emission collected at 425−475 nm; the fluorescence of MitoTracker Green, BODIPY, and GFP was excited with a 488 nm laser with emission collected at 500−600 nm. The fluorescence of HQO was excited with 559 and 635 nm lasers, and the emission was collected at 570−610 and 650−730 nm, respectively. The images were postprocessed with Olympus FV10-ASW 1.6 viewer software.

Real-Time Live Cell Confocal Imaging. Cells were seeded in confocal dishes with 10^5 cells per dish and cultured for attachment. Cells were washed with PBS (pH 7.4) three times before imaging. Cells were treated with 1 mL of serum-free culture media containing 20 μM HQO and placed into a live cell incubator. The fluorescence images were taken immediately and at 5 min, 10 min, 20 min, 30 min, 1 h, 2 h, 3 h, and 4 h incubation time points with excitation at 559 and 635 nm and emission at 570−610 and 650−730 nm.

■ ASSOCIATED CONTENT

Supporting Information

The Supporting Information is available free of charge on the ACS Publications website at DOI: 10.1021/jacs.6b04048.

Scheme showing the synthesis of HQO; figures showing absorption spectra, ^{1}H-NMR titration, fluorescence spectra, cytotoxicity, confocal images, etc.; tables showing molar extinction coefficients, apparent pK_a values, and CMCs (PDF)

■ AUTHOR INFORMATION

Corresponding Author

*sgdh@iccas.ac.cn

Author Contributions

#Y.L., J.Z., L.W.: These authors contributed equally.

Notes

The authors declare no competing financial interest.

DOI: 10.1021/jacs.6b04048
J. Am. Chem. Soc. 2016, 138, 12368−12374

■ ACKNOWLEDGMENTS

We gratefully acknowledge the financial support from Grant 973 Program (2013CB933700) and NSF of China (grants 21275149, 21375135, 21575147, 21535009, and 21321003).

■ REFERENCES

(1) (a) Newmeyer, D. D.; Ferguson-Miller, S. *Cell* **2003**, *112* (4), 481−490. (b) Chan, D. C. *Cell* **2006**, *125* (7), 1241−1252. (c) McBride, H. M.; Neuspiel, M.; Wasiak, S. *Curr. Biol.* **2006**, *16* (14), R551−R560. (d) Stotland, A.; Gottlieb, R. A. *Biochim. Biophys. Acta, Mol. Cell Res.* **2015**, *1853* (10), 2802−2811.

(2) Wallace, D. C. *Annu. Rev. Genet.* **2005**, *39*, 359−407.

(3) Kanki, T.; Furukawa, K.; Yamashita, S. *Biochim. Biophys. Acta, Mol. Cell Res.* **2015**, *1853* (10), 2756−2765.

(4) (a) Luzio, J. P.; Pryor, P. R.; Bright, N. A. *Nat. Rev. Mol. Cell Biol.* **2007**, *8* (8), 622−632. (b) Kroemer, G.; Jaattela, M. *Nat. Rev. Cancer* **2005**, *5* (11), 886−897.

(5) (a) Mizushima, N.; Yoshimori, T.; Levine, B. *Cell* **2010**, *140* (3), 313−326. (b) Dolman, N. J.; Chambers, K. M.; Mandavilli, B.; Batchelor, R. H.; Janes, M. S. *Autophagy* **2013**, *9* (11), 1653−1662. (c) Xie, R.; Nguyen, S.; McKeehan, W. L.; Liu, L. Y. *BMC Cell Biol.* **2010**, *11*, 89.

(6) (a) Klionsky, D. J.; Abdalla, F. C.; Abeliovich, H.; Abraham, R. T.; Acevedo-Arozena, A.; Adeli, K.; et al. *Autophagy* **2012**, *8* (4), 445−544. (b) Du, Y.; Wang, X. G.; Wang, B.; Chen, W. J.; He, R. J.; Zhang, L.; Xing, X. P.; Su, J. M.; Wang, Y. S.; Zhang, Y. *Mol. Reprod. Dev.* **2014**, *81* (11), 1042−1052. (c) Warnes, G. *Methods* **2015**, *82*, 21−28. (d) Kim, I.; Lemasters, J. J. *Am. J. Physiol-Cell Ph* **2011**, *300* (2), C308−C317.

(7) Rodriguez-Enriquez, S.; Kim, I.; Currin, R. T.; Lemasters, J. J. *Autophagy* **2006**, *2* (1), 39−46.

(8) (a) Capodilupo, A. L.; Vergaro, V.; Fabiano, E.; De Giorgi, M.; Baldassarre, F.; Cardone, A.; Maggiore, A.; Maiorano, V.; Sanvitto, D.; Gigli, G.; Ciccarella, G. *J. Mater. Chem. B* **2015**, *3* (16), 3315−3323. (b) Lim, C. S.; Hong, S. T.; Ryu, S. S.; Kang, D. E.; Cho, B. R. *Chem. - Asian J.* **2015**, *10* (10), 2240−2249. (c) Yang, W. G.; Chan, P. S.; Chan, M. S.; Li, K. F.; Lo, P. K.; Mak, N. K.; Cheah, K. W.; Wong, M. S. *Chem. Commun.* **2013**, *49* (33), 3428−3430.

(9) (a) Zhang, C.; Liu, T.; Su, Y. P.; Luo, S. L.; Zhu, Y.; Tan, X.; Fan, S.; Zhang, L. L.; Zhou, Y.; Cheng, T. M.; Shi, C. M. *Biomaterials* **2010**, *31* (25), 6612−6617. (b) Tan, X.; Luo, S. L.; Wang, D. C.; Su, Y. P.; Cheng, T. M.; Shi, C. M. *Biomaterials* **2012**, *33* (7), 2230−2239. (c) Zhang, E. L.; Luo, S. L.; Tan, X.; Shi, C. M. *Biomaterials* **2014**, *35* (2), 771−778.

(10) (a) Guo, Z. Q.; Nam, S.; Park, S.; Yoon, J. *Chem. Sci.* **2012**, *3* (9), 2760−2765. (b) Kim, Y. M.; Choi, Y. D.; Weissleder, R.; Tung, C. H. *Bioorg. Med. Chem. Lett.* **2007**, *17* (18), 5054−5057. (c) Strekowski, L.; Mason, J. C.; Lee, H.; Say, M.; Patonay, G. *J. Heterocycl. Chem.* **2004**, *41* (2), 227−232. (d) Mason, J. C.; Patonay, G.; Strekowski, L. *Heterocycl. Commun.* **1997**, *3* (5), 409−411.

(11) (a) Luo, S. J.; Jiang, X. B.; Zou, L.; Wang, F.; Yang, J. F.; Chen, Y. M.; Zhao, J. *Macromolecules* **2013**, *46* (8), 3132−3136. (b) Crans, D. C.; Levinger, N. E. *Acc. Chem. Res.* **2012**, *45* (10), 1637−1645.

(12) (a) Yamamoto, A.; Tagawa, Y.; Yoshimori, T.; Moriyama, Y.; Masaki, R.; Tashiro, Y. *Cell Struct. Funct.* **1998**, *23* (1), 33−42. (b) Klucken, J.; Poehler, A. M.; Ebrahimi-Fakhari, D.; Schneider, J.; Nuber, S.; Rockenstein, E.; Schlotzer-Schrehardt, U.; Hyman, B. T.; McLean, P. J.; Masliah, E.; Winkler, J. *Autophagy* **2012**, *8* (5), 754−766.

(13) Perry, S. W.; Norman, J. P.; Barbieri, J.; Brown, E. B.; Gelbard, H. A. *BioTechniques* **2011**, *50* (2), 98−115.

(14) (a) Schlame, M.; Brody, S.; Hostetler, K. Y. *Eur. J. Biochem.* **1993**, *212* (3), 727−735. (b) Corcelli, A.; Schlame, M. *Eur. J. Lipid Sci. Technol.* **2013**, *115* (12), 1501−1503.

(15) Zhou, J.; Li, G. B.; Zheng, Y.; Shen, H. M.; Hu, X.; Ming, Q. L.; Huang, C.; Li, P.; Gao, N. *Autophagy* **2015**, *11* (8), 1259−1279.

DOI: 10.1021/jacs.6b04048
J. Am. Chem. Soc. 2016, 138, 12368−12374